acta acustica 2 (1994) 101-112 April 1994, page 101

Computation of subsonic and supersonic jet mixing noise using a modified $k - \epsilon$ model for compressible free shear flows

C. Bailly[1], P. Lafon[1] and S. Candel[2]

[1] Direction des Etudes et Recherches d'Electricité de France, 1 Avenue du Général de Gaulle, 92141 Clamart Cedex, France
[2] Ecole Centrale Paris, 92295 Châtenay-Malabry Cedex, France

(Received 2 April 1993; revised 24 November 1993; accepted 15 March 1994)

Abstract. – This study deals with the numerical determination of subsonic and supersonic jet mixing noise. An analytic expression for the acoustic intensity can be deduced from Lighthill's analogy (1952, 1954). Ribner (1969) proposed a modeling of the Lighthill stress tensor for an isotropic turbulence description, and Goldstein & Rosenbaum (1973) have developed a similar approach for an axisymmetric turbulence description. In these models, some variables remain unknown and are usually expressed by using empirical or dimensional considerations. Instead of following this approach, we locally deduce these quantities from aerodynamic results, which are the mean velocity, the turbulent kinetic energy k and the dissipation rate ϵ. Aerodynamic computations are performed by using a $k - \epsilon$ turbulent code, modified for compressible free shear flows. Thus, intensity, spectrum and power of the radiated acoustic field are numerically calculated for subsonic and supersonic free jets ($0.56 \leq M \leq 2.0$). The comparison between these numerical results and experimental data shows the predictive capability of the two models, except when refraction effects are not negligible.

Pacs numbers: 43.28Ra.

1. Introduction

Lighthill's theory (1952, 1954) formulated from the fundamental equations of motion uses an analogy to calculate the acoustic radiation from a limited volume of turbulent fluid embedded in an infinite homogeneous medium at rest. The acoustic fluctuations generated by the turbulent flow are equivalent to the acoustic fluctuations generated by a quadrupole distribution of strengh T_{ij} in a fictitious homogeneous domain at rest. The T_{ij} tensor is stochastic and can normally be defined only in a statistical sense. However, the governing wave equation is so simple that the mean square sound pressure field can be expressed in terms of a double integral of the two point space-time correlations of T_{ij} (Crighton, 1975; Goldstein, 1976).

Using assumed correlations in an approximate form of T_{ij}, Proudman (1952), Ribner (1964, 1969), Pao & Lowson (1970), Goldstein & Rosenbaum (1973) proposed explicit formulations for turbulence generated aerodynamic noise. The models defined in these studies require statistical informations about the turbulence. These quantities are usually obtained by means of empirical or dimensional considerations.

Over the years different methods have been devised to directly include the flow effects on the radiated noise. In the development due to Phillips (1960), the Lighthill equation is replaced by an inhomogeneous wave equation for a moving medium with the mean flow effects appearing in the wave operator rather than in the T_{ij} source term. However, the formulation devised by Phillips does not exhibit an exact wave operator in a moving medium as pointed out by Lilley (1972) and Doak (1972). From Phillips'equation, Lilley deduced a third order wave equation to further separate propagation terms and source terms. Much work has been expended in order to solve Lilley's equation for uniform and non uniform mean flows. Many of these studies deal with the propagation of acoustic waves due to monopolar or quadrupolar source terms. The analytical solutions derived are rather sophisticated and lack generality. The sound generation models are also rather specialized. Being analytically and numerically much more difficult to apply than the Lighthill based formalisms, the added labor has not yet paid off in predictive capability. However the work done on this problem has enhanced the current understanding of aerodynamic noise generation and propagation.

In general the technical literature dealing with jet noise is quite extensive and one can find detailed investigations of the physics of sound generation in turbulent shear flows. Many studies deal with the mechanisms of noise generation, the influence of the organized structure of turbulence, the propagation of the sound waves from the noise sources through the jet flow. The number of studies which consider the computation of the sound radiated from the basic aerodynamic field is much smaller. The new possibilities offered by modern computational fluid dynamics have not been extensively used for noise estimation. This aspect is adressed in the preset article.

For this, we will use a method for aerodynamic noise estimation based on the studies of Ribner (1969), and Goldstein & Rosenbaum (1973) and proposed in Béchara (1992) and Béchara et al. (1992, 1993). In the present article we generalize this approach to subsonic and supersonic jet flows. The key idea is to use Reynolds average Navier-Stokes computations based on a modified $k-\epsilon$ model for compressible free shear flows in order to deduce statistical informations about the turbulence from local aerodynamic computations and then use these informations to evaluate the aerodynamic noise sources. We will specifically consider cold free jets exhausting from a circular nozzle into an atmosphere at rest. We assume that for supersonic Mach numbers, the jet is adapted (i.e. that it does not contain shocks). A brief presentation of Lighthill's theory is given in Section 2. In Sections 3 and 4, the noise generation models due to Ribner and Goldstein et al. are reviewed. Aerodynamic results for subsonic and supersonic cold round free jets are described in Section 5. Finally, comparison between acoustical results and experimental data is carried out in Section 6.

2. Lighthill's theory

From the fundamental equations of motion, Lighthill (1952, 1954) has shown that the density fluctuations observed at a point $\mathbf{x}$ in the far field, and generated by a limited volume V of turbulent fluid (see Figure 1), are given by:

$$(\rho-\rho_o)(\mathbf{x},t) = \frac{1}{4\pi c_o^4}\frac{x_i x_j}{x^3} \times \int_V \frac{\partial^2}{\partial t^2} T_{ij}\left(\mathbf{y}, t-\frac{|\mathbf{x}-\mathbf{y}|}{c_o}\right) \mathrm{d}\mathbf{y} \quad (1)$$

with

$$T_{ij} = \rho u_i u_j + \left((p-p_o) - c_o^2(\rho-\rho_o)\right)\delta_{ij} - \tau_{ij} \quad (2)$$

where T_{ij} is the instantaneous Lighthill's stress tensor. The source term T_{ij} can be replaced by the instantaneous Reynolds tensor $\rho u_i u_j$, for high Reynolds number flows without entropy fluctuations. Furthermore, the density in the source term is approximated by ρ_o if the Mach number is not too large, i.e. $M \leq 2$. With these assumptions, the T_{ij} tensor is finally reduced to $\rho_o u_i u_j$. Assuming a stationnary turbulence, one may define the autocorrelation function of the pressure C_{pp}:

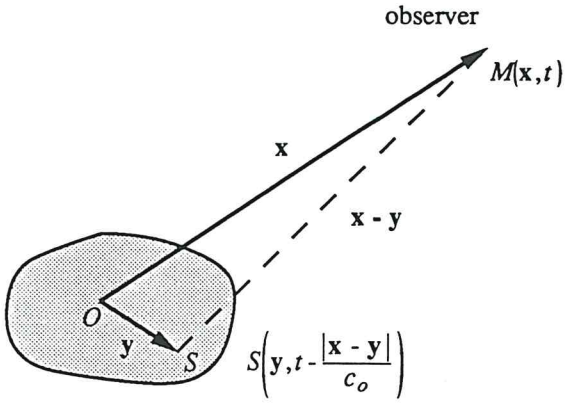

Figure 1. Geometry of sound source radiation.

$$C_{pp}(\mathbf{x},\tau) = \frac{\overline{[p(\mathbf{x},t)-p_o]\,[p(\mathbf{x},t+\tau)-p_o]}}{\rho_o c_o} \quad (3)$$

In agreement with standard aeroacoustic studies the correlation function is normalised by $\rho_o c_o$. With this convention the correlation function evaluated for $\tau = 0$ is equal to the acoustic intensity (when the observation point $\mathbf{x}$ is in the far field). Inserting relation (1) in equation (3), the function C_{pp} takes the following form in the far field:

$$C_{pp}(\mathbf{x},\tau) = \frac{\rho_o}{16\pi^2 c_o^5 x^2}\frac{x_i x_j x_k x_l}{x^4} \times \frac{\partial^4}{\partial \tau^4}\int\!\!\int_V R_{ijkl}\left(\mathbf{y},\boldsymbol{\eta},\tau+\frac{\mathbf{x}.\boldsymbol{\eta}}{c_o x}\right) d\mathbf{y}\,d\boldsymbol{\eta} \quad (4)$$

with

$$R_{ijkl}(\mathbf{y},\boldsymbol{\eta},\tau) = \frac{\overline{[T_{ij}(\mathbf{y},t)\,T_{kl}(\mathbf{y}+\boldsymbol{\eta},t+\tau)]} - \varphi_{ijkl}(\mathbf{y},\boldsymbol{\eta})}{\rho_o^2}$$

where R_{ijkl} is the fourth-order space-time velocity correlation tensor, and φ_{ijkl} designates an arbitrary tensor independant of τ. This last tensor is selected so that the mean value of $R_{ijkl}(\mathbf{y},\boldsymbol{\eta},0)$ equals zero. Thus, two waves emitted at the same time by two source points separated by the vector $\boldsymbol{\eta}$ in V, are observed at the point $\mathbf{x}$ and at times t and $t+\Delta t$, where the retarded time Δt is equal to $\mathbf{x}.\boldsymbol{\eta}/c_o x$.

However, in the equation (4), the time τ in the correlation tensor $R_{ijkl}(\mathbf{y},\mathbf{0},\tau)$ represents the crossing time of a convected eddy rather than the characteristic decay

time of the turbulence. It is then convenient to introduce a moving reference frame, to take into account convection effects (Fflowcs Williams, 1963; Crighton, 1975; Goldstein, 1976):

$$\xi = \eta - U_c \tau \mathbf{y_1} \tag{5}$$

and the new correlation tensor is such that:

$$\mathcal{R}_{ijkl}(\mathbf{y}, \xi, \tau) = R_{ijkl}(\mathbf{y}, \eta, \tau) \tag{6}$$

In this frame, which moves with the mean convection velocity of eddies, the decay time of turbulence is maximum. Hence, the retarded time compared to this decay time may be neglected and $\mathcal{R}_{ijkl}(\mathbf{y}, \xi, \tau)$ changes very slowly during the period $\mathbf{x}.\xi/c_o x$. Thus, equation (4) becomes:

$$C_{pp}(\mathbf{x}, \tau) = \frac{\rho_o}{16\pi^2 c_o^5 x^2} \frac{x_i x_j x_k x_l}{x^4} \frac{1}{C^5} \times \int\int_V \frac{\partial^4}{\partial t^4} [\mathcal{R}_{ijkl}(\mathbf{y}, \xi, t)]_{t=\frac{\tau}{C}} \mathrm{d}\mathbf{y}\mathrm{d}\xi \tag{7}$$

where $C = 1 - M_c \cos\theta$ designates the convection factor, and θ represents the angle between the mean flow direction $\mathbf{y_1}$ and the direction of the observer located at point $\mathbf{x}$ (see Figure 2).

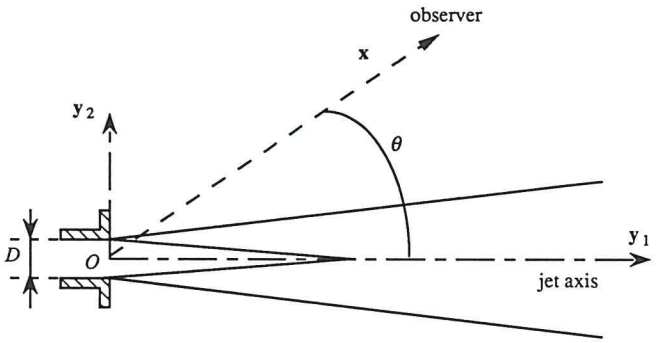

Figure 2. Sketch of the jet flow configuration.

3. Ribner model

Ribner (1964, 1969) has developed a formulation of the noise generation from the Lighthill's theory with the following assumptions. The velocity field is described as the sum of a local mean flow component U in the $\mathbf{y_1}$ direction and a turbulent fluctuating component u_t with zero mean:

$$u_i = U\delta_{1i} + u_{ti} \tag{8}$$

Inserting this decomposition (8) into the space-time correlation tensor $\mathcal{R}_{ijkl}$, and assuming that the turbulence is locally homogeneous and isotropic, $\mathcal{R}_{ijkl}$ can be written in the form:

$$\begin{aligned}\mathcal{R}_{ijkl} = {} & \overline{u'_{ti}u'_{tj}u''_{tk}u''_{tl}} \\ & + U'U''(\delta_{1i}\delta_{1k}\overline{u'_{tj}u''_{tl}} + \delta_{1j}\delta_{1k}\overline{u'_{ti}u''_{tl}} \\ & + \delta_{1i}\delta_{1l}\overline{u'_{tj}u''_{tk}} + \delta_{1j}\delta_{1l}\overline{u'_{ti}u''_{tk}})\end{aligned} \tag{9}$$

With reference to the terminology introduced by Lilley (1958), the first term is called the self-noise contribution (contribution arising from turbulence alone), and the second term is called the shear-noise contribution (interaction between turbulence and mean flow). Morever, if one assumes a normal joint probability of the variables u'_t and u''_t, the self-noise contribution can be expressed as follows (Batchelor, 1953):

$$\begin{aligned}\overline{u'_{ti}u'_{tj}u''_{tk}u''_{tl}} = {} & \overline{u'_{ti}u'_{tj}}\,\overline{u''_{tk}u''_{tl}} \\ & + \overline{u'_{ti}u''_{tk}}\,\overline{u'_{tj}u''_{tl}} + \overline{u'_{ti}u''_{tl}}\,\overline{u'_{tj}u''_{tk}}\end{aligned} \tag{10}$$

If one postulates that the two-point velocity tensor $\mathcal{R}_{ij}$ is the product of a time factor by a space factor, and if one assumes that the turbulence is isotropic, it is possible to write the correlation tensor in the form (Hinze, 1975):

$$\mathcal{R}_{ij}(\mathbf{y}, \xi, \tau) = \mathrm{e}^{-\omega_f^2 \tau^2} \mathcal{R}_{ij}(\mathbf{y}, \xi) \tag{11}$$

$$\mathcal{R}_{ij}(\mathbf{y}, \xi) = \overline{u_t^2} \left[\left(f + \frac{1}{2}\xi \frac{\mathrm{d}f}{\mathrm{d}\xi} \right) \delta_{ij} - \frac{1}{2} \frac{\mathrm{d}f}{\mathrm{d}\xi} \frac{\xi_i \xi_j}{\xi} \right] \tag{12}$$

where the longitudinal correlation function f is taken to be:

$$f(\xi) = \mathrm{e}^{-\frac{\pi\xi^2}{L^2}} \tag{13}$$

In expressions (11) (12) and (13) the coordinate system is cartesian, L is the longitudinal integral scale of turbulence, ω_f the characteristic angular frequency and $\overline{u_t^2}$ is equal to $2/3\,k$, where k is the turbulent kinetic energy.

To evaluate the product of mean velocities $U'U''$, one may use a Taylor expansion around the point $\mathbf{y} + \frac{1}{2}\xi$, and obtain:

$$\begin{aligned}U'U'' &= U\left(y_2 - \frac{1}{2}\xi_2\right) U\left(y_2 + \frac{1}{2}\xi_2\right) \\ &= U^2(y_2) - \frac{1}{4}\xi_2^2 \left[\frac{\partial U}{\partial y_2}\right]^2 + \text{other terms}\end{aligned} \tag{14}$$

Finally, using expressions (8) to (13) and the axisymmetric property of the autocorrelation function C_{pp}, the integration (7) for $\tau = 0$ provides the directional intensity $I = I^{\text{Self-noise}} + I^{\text{Shear-noise}}$ radiated from an unit source

volume located at $\mathbf{y}$:

$$I^{\text{Self-noise}}(\mathbf{x} \mid \mathbf{y}) = \frac{3}{2\sqrt{2}} \frac{\rho_o \overline{u_t^2}^2 L^3}{\pi^2 c_o^5 x^2} \frac{1}{C^5} \omega_f^4 \tag{15}$$

$$I^{\text{Shear-noise}}(\mathbf{x} \mid \mathbf{y}) = \\ = \frac{3}{8} \frac{\rho_o \overline{u}_t^2 L^5}{\pi^3 c_o^5 x^2} \left(\frac{\partial U}{\partial y_2}\right)^2 \frac{1}{C^5} \omega_f^4 D_{\text{Ribner}}^{\text{Shear-noise}} \tag{16}$$

$$D_{\text{Ribner}}^{\text{Shear-noise}} = \frac{1}{2}\left(\cos^4\theta + \cos^2\theta\right)$$

From these expressions one finds that the self-noise contribution has an isotropic directivity, which is a direct consequence of the isotropic description of the turbulence. The total intensity takes the compact form:

$$I(\mathbf{x} \mid \mathbf{y}) = \frac{1}{C^5}\left[A + \frac{B}{2}\left(\cos^4\theta + \cos^2\theta\right)\right]$$

This expression exibits the influence of convection which enhances the radiated acoustic intensity in the downstream direction. However, this simplified expression of the convection factor C has a singularity at high Mach numbers. A more sophisticated analysis developped by Ffowcs Williams (1960, 1963) and taking into account the changes of retarded time with source position leads to a modified convection factor C_m given by:

$$C_m = \left[\left(1 - M_c \cos\theta\right)^2 + \frac{\omega_f^2 L^2}{\pi c_o^2}\right]^{\frac{1}{2}} \\ = \left[\left(1 - M_c \cos\theta\right)^2 + \alpha^2 M_c^2\right]^{\frac{1}{2}} \tag{17}$$

where α is a constant. An expression for the power spectral density can be deduced by a Fourier transform of expression (7). One may write :

$$S_{pp}^{\text{Self-noise}}(\mathbf{x} \mid \mathbf{y}, \omega) = \frac{\rho_o \overline{u_t^2}^2 L^3}{128\pi^2\sqrt{\pi} c_o^5 x^2} \frac{\omega^4}{\omega_f} e^{-\frac{C^2\omega^2}{8\omega_f^2}} \tag{18}$$

$$S_{pp}^{\text{Shear-noise}}(\mathbf{x} \mid \mathbf{y}, \omega) = \frac{\rho_o \overline{u}_t^2 L^5}{64\pi^3\sqrt{\pi} c_o^5 x^2} \\ \times \left(\frac{\partial U}{\partial y_2}\right)^2 \frac{\omega^4}{\omega_f} e^{-\frac{C^2\omega^2}{4\omega_f^2}} D_{\text{Ribner}}^{\text{Shear-noise}} \tag{19}$$

4. Goldstein and Rosenbaum model

Goldstein & Rosenbaum (1973) have developed a similar approach for an axisymmetric description of the turbulence. Indeed, the mean flow introduces a preferred direction $\mathbf{y_1}$ for the turbulent fluctuations. For example, Davies et al. (1963) noticed a reduction by a factor 3 of the transverse integral scale L_2 of the turbulence with regard to L_1 . As a consequence, the non isotropic structure of the turbulence can have an important effect on the directivity pattern (Ribner, 1969).

For an axisymmetric turbulence, the two-point correlation tensor $\mathcal{R}_{ij}(\mathbf{x}, \boldsymbol{\xi})$ is given in cartesian coordinate by:

$$\begin{aligned} \mathcal{R}_{ij} &= \epsilon_{jlm} \frac{\partial q_{im}}{\partial \xi_l} \\ \epsilon_{jlm} &= \frac{1}{2}(j-l)(l-m)(m-j) \\ q_{ij} &= \xi_k \left[\epsilon_{ijk} Q_1 + \epsilon_{i1k}\left(\delta_{1j} Q_2 + \xi_j Q_3\right)\right] \\ Q_3 &= \left(\frac{\partial}{\partial \xi_1} - \frac{\xi_1}{\xi_3}\frac{\partial}{\partial \xi_3}\right) Q_1 \end{aligned} \tag{20}$$

The scalar functions Q_1 and Q_2 are selected with the same assumptions as in Ribner's model: the two-point correlation tensor is written as a product of a time factor by a space factor. The following choice is kinematically acceptable:

$$\begin{aligned} Q_1(\mathbf{y}, \boldsymbol{\xi}, \tau) &= -\frac{1}{2}\overline{u_{t1}^2} f(\mathbf{y}, \tau) \exp\left\{-\left(\frac{\xi_1^2}{L_1^2} + \frac{\xi_2^2}{L_2^2}\right)^{1/2}\right\} \\ Q_2(\mathbf{y}, \boldsymbol{\xi}, \tau) &= -\left(\overline{u_{t2}^2} - \overline{u_{t1}^2}\right) f(\mathbf{y}, \tau) \\ &\quad \times \exp\left\{-\left(\frac{\xi_1^2}{L_1^2} + \frac{\xi_2^2}{L_2^2}\right)^{1/2}\right\} \end{aligned} \tag{21}$$

with

$$f(\mathbf{y}, \tau) = e^{-\omega_f^2 \tau^2} \tag{22}$$

Thus, by integration over the source volume, one obtains the following expression for the acoustic intensity:

$$I^{\text{Self-noise}}(\mathbf{x} \mid \mathbf{y}) = \frac{12}{5\pi} \frac{\rho_o \overline{u_{t1}^2}^2 L_1 L_2^2}{c_o^5 x^2} \frac{1}{C^5} \omega_f^4 D_{\text{Goldstein}}^{\text{Self-noise}} \tag{23}$$

$$I^{\text{Shear-noise}}(\mathbf{x} \mid \mathbf{y}) = \\ = \frac{24}{\pi} \frac{\rho_o \overline{u_{t1}^2} L_1 L_2^4}{c_o^5 x^2} \left(\frac{\partial U}{\partial y_2}\right)^2 \frac{1}{C^5} \omega_f^4 D_{\text{Golstein}}^{\text{Shear-noise}} \tag{24}$$

where

$$\begin{aligned} D_{\text{Goldstein}}^{\text{Self-noise}} &= 1 + 2\left(\frac{M}{9} - N\right)\cos^2\theta \sin^2\theta \\ &\quad + \frac{1}{3}\left[\frac{M^2}{7} + M - \frac{3N}{2}\right. \\ &\quad \left. \times \left(3 - 3N + \frac{3}{2\Delta^2} - \frac{\Delta^2}{2}\right)\right] \sin^4\theta \\ D_{\text{Goldstein}}^{\text{Shear-noise}} &= \cos^2\theta\left[\cos^2\theta + \frac{1}{2}\left(\frac{1}{\Delta^2} - 2N\right)\sin^2\theta\right] \end{aligned}$$

and

$$\Delta = \frac{L_2}{L_1}, \quad M = \left[\frac{3}{2}\left(\Delta - \frac{1}{\Delta}\right)\right]^2, \quad N = 1 - \frac{\overline{u_{t2}^2}}{\overline{u_{t1}^2}}$$

Because of the axisymmetric description of the turbulence, the self-noise also features an angular dependence. The radiation pattern has a dipole shape with a dipole axis perpendicular to the mean flow direction. It is interesting to notice that in the case of an isotropic turbulence ($\Delta = 1, M = N = 0$), $D_{\text{Goldstein}}^{\text{Self-noise}} = 1$.

Like for Ribner's model, an expression of the power spectral density can be deduced by Fourier transformation of the correlation function:

$$S_{\text{pp}}^{\text{Self-noise}}(\mathbf{x} \mid \mathbf{y}, \omega) = \frac{1}{40\sqrt{2\pi}} \frac{\rho_o \overline{u_{t1}^2}^2 L_1 L_2^2}{\pi c_o^5 x^2} \frac{\omega^4}{\omega_f} \times e^{-\frac{c^2\omega^2}{8\omega_f^2}} D_{\text{Goldstein}}^{\text{Self-noise}} \quad (25)$$

$$S_{\text{pp}}^{\text{Shear-noise}}(\mathbf{x} \mid \mathbf{y}, \omega) = \frac{1}{\sqrt{\pi}} \frac{\rho_o \overline{u_{t1}^2} L_1 L_2^4}{\pi c_o^5 x^2} \times \left(\frac{\partial U}{\partial y_2}\right)^2 \frac{\omega^4}{\omega_f} e^{-\frac{c^2\omega^2}{4\omega_f^2}} D_{\text{Goldstein}}^{\text{Shear-noise}} \quad (26)$$

5. Application of the two models to jet noise prediction

At this point it is worth summarizing the various steps and approximations which lead to the final model.

1. The acoustic model is based on the Lighthill's analogy. The stress tensor $\rho_o u_i u_j$ is decomposed in terms of a mean velocity and a fluctuating component. It is assumed that the velocity fluctuations have a gaussian probability density function. The computation of the far sound field requires a knowledge of the mean aerodynamic field and a model for the space-time correlation of the velocity fluctuations.
2. To get these informations, one uses average mean flow equations together with a $k - \epsilon$ closure scheme. The mean aerodynamic flow, the local length scale, convection velocity and characteristic frequency are determined from the calculations.
3. The $k - \epsilon$ aerodynamic model does not provide the space-time correlation function which is determined by making use of additional assumptions (isotropic turbulence or axisymetric turbulence, gaussian shape for the correlation function, Taylor hypothesis for convected turbulence fluctuations).

A complete model is obtained in this way and it is used in this article to calculate different jet noise radiation problems.

5.1. *Aerodynamic results*

The aerodynamic results are obtained from a numerical solution of Reynolds average Navier-Stokes equations associated with a $k - \epsilon$ model. These calculations are carried out with an axisymmetric compressible version of the code ESTET developed by the "Laboratoire National Hydraulique" of the "Direction des Etudes et Recherches d'Electricité de France" (see appendix). We account for compressibility effects on the turbulence, by introducing an energy dissipation resulting from dilatation processes into the standard $k - \epsilon$ model (see Zeman, 1990 for instance). Computations are made for unheated free jets at nominal Mach numbers of 0.56, 0.86, 1.33, 1.48, 1.67 and 2.0. Numerical results are compared with several groups of experimental data (Davies et al., 1963; Lau et al., 1979; Nagamatsu et al., 1970; Seiner et al., 1982).

Figures 3 and 4 respectively display Mach number contour plots and spatial distributions of the turbulent kinetic energy k for two nominal Mach numbers of 0.86 and 2.0. The computation domain has $20D$ in the axial direction, with a nozzle diameter D of 0.025 m. The length of the potentiel core X_c (i.e. the length where the mean center-line velocity is constant) is about $6D$ for the subsonic jet and $9.6D$ for the supersonic jet, which is close to the experimentally observed values of $5D$ (Nagamatsu et al., 1970) and $10D$ (Seiner et al., 1982). The jet mixing layers corresponding to the maximum of turbulent energy k may be identified in Figure 4. The production of k is directly associated with velocity gradients, which reach a maximum in the mixing layers and are negligible in the potentiel core. The growth of the length of the potentiel core in the supersonic case induces thinner mixing layers. Figure 5a demonstrates the close agreement between the mean center-line Mach number and experimental data of Seiner et al. (1982) for the nominal Mach number of 2.0. The small bulges observed in this case are due to a slight mismatch between the jet exhaust pressure and the ambiant pressure. Comparison of velocity profiles with experimental data for different axial locations are reported in Figure 5b. Other comparisons, based on the radial intensity profiles and the longitudinal integral scale of the turbulence are not shown in this paper, but indicate that suitable numerical predictions are indeed obtained.

5.2. *Acoustic source modeling and results*

In order to use expressions of Ribner's model and Goldstein's model, it is necessary to specify the statistical variables which appear in these formulations. Thus, from the aerodynamic computation, we utilize the following closure relations:

1. The characteristic angular frequency of the turbulence is given by:

$$\omega_f \sim 2\pi \frac{\epsilon}{k}$$

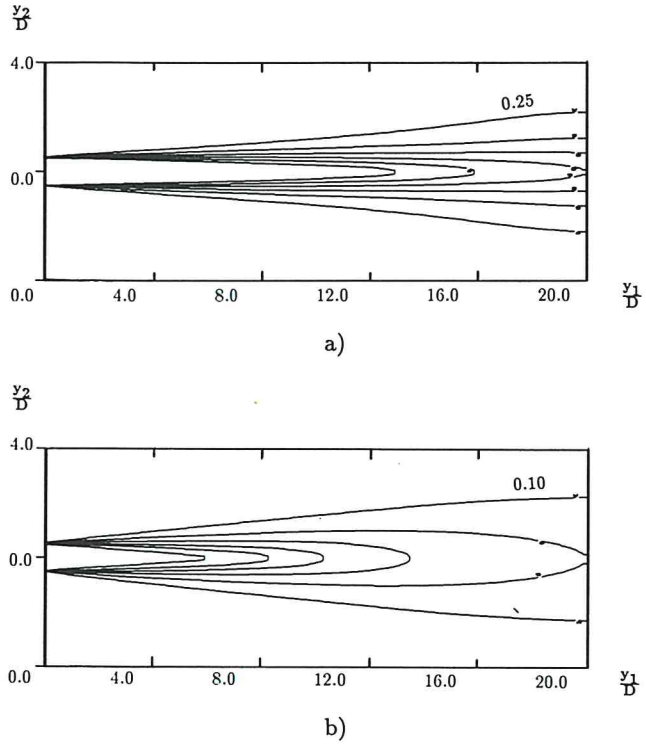

Figure 3. Mach number contour plot. (a) $M = 2.0$. Six isolines from 0.25 to 1.75 with a step of 0.3. (b) $M = 0.86$. Six isolines from 0.1 to 0.85 with a step of 0.15.

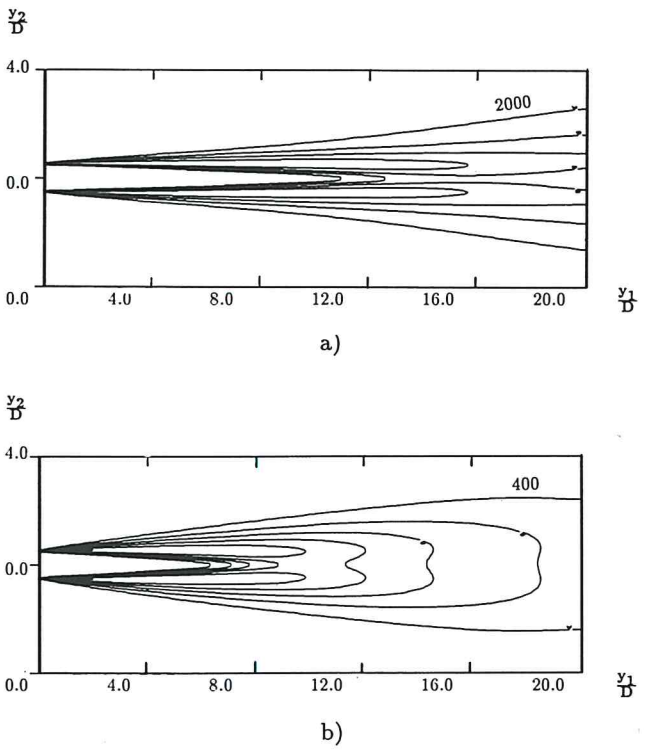

Figure 4. Turbulent kinetic energy contour plot. (a) $M = 2.0$. Six isolines from 2000 to 12000 $m^2.s^{-2}$ with a step of 2000 $m^2.s^{-2}$. (b) $M = 0.86$. Six isolines from 400 to 3900 $m^2.s^{-2}$ with a step of 500 $m^2.s^{-2}$.

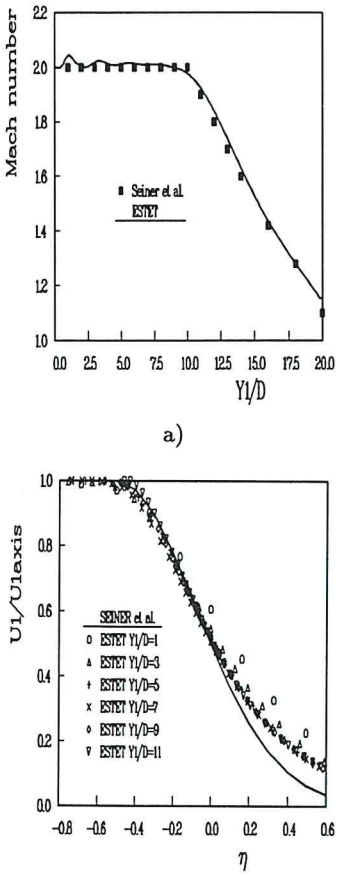

Figure 5. Aerodynamic profiles for a nominal Mach number of $M = 2.0$. (a) Mean center-line Mach number. (b) Radial velocity profiles at different locations. $\frac{U_1}{U_{1\text{axis}}} = f(\eta)$ with $\eta = \frac{y_2 - y_2(0.5)}{\delta} y_2(0.5)$ is the radial location where the velocity equals $U_1 = 0.5 U_{1\text{axis}}$, where $U_{1\text{axis}}$ is the velocity on the center line of the jet at the given y_1 location, and δ is the local shear layer thickness $\delta = y_2(0.1) - y_2(0.9)$, which represents the radial distance between the points where the local velocity is $U_1 = 0.1 U_{1\text{axis}}$ and $U_1 = 0.9 U_{1\text{axis}}$.

2. From the concept of turbulent viscosity, the axial and radial kinetic energy are determined from:

$$\overline{u_{t1}^2} = \frac{2}{3}k - 2\nu_t \frac{\partial \overline{U_1}}{\partial x_1}$$

$$\overline{u_{t2}^2} = \frac{2}{3}k - 2\nu_t \frac{\partial \overline{U_2}}{\partial x_2}$$

where ν_t is the kinematic turbulent viscosity.

3. Integral length scales of turbulence should be determined from spectral considerations. However, numerical simulations indicate that the longitudinal integral scale can be approximated by the expression:

$$L_1 \sim \frac{k^{2/3}}{\epsilon}$$

The $k-\epsilon$ model based on the concept of turbulent viscosity is unable to correctly represent a transverse in-

tegral scale. Thus, we impose a value determined from experiments by Davies et al. (1963): $L_2 = L_1/3$. This accounts for the anisotropy of the turbulence length scales, a characteristic of free jet flows.

4. The convection velocity U_c cannot be directly deduced from our aerodynamic calculations. This velocity is often (Lush, 1971; Ribner, 1969; Tanna, 1977) considered as a constant throughout the jet, and equals 0.6 - 0.7 times the mean jet exit velocity. However, Davies et al. (1963) have measured the radial profile of U_c in the mixing region of a subsonic jet. From these two results, we calculate in this paper the convection velocity as $0.67U_{1\text{axis}}$ where $U_{1\text{axis}}$ is the mean velocity on the jet axis in the local Section.

Finally, the relations used to model the three quantities ω_f, L_1 and L_2, depend implicitly on unknown scaling constants. For this reason, a global adjustment factor is introduced in the intensity expression of the Ribner and Goldstein models. For each of the two models, this factor is determinated so that acoustical intensity at $\theta = 90°$ and for the exit Mach number $M = 0.56$, coincides with the experimental value of Lush (1971). In other words, the acoustical intensity for a nominal Mach number $M = 0.56$, and an observation angle $\theta = 90°$, is taken as a reference. The two global adjustement factors determined in this way are used for all other flow configurations.

5.2.1. *Acoustic power*

Figure 6a shows the acoustic power for the two models, and for a range of nominal Mach numbers ranging from 0.56 to 2.0. Power levels are expressed in dB with a reference of 10^{-13} W, and per unit of nozzle area. The same figure also shows experimental data of selected articles published by Lush (1971), Tanna (1977), Norum & Seiner (1982), Seiner (1982), Yu & Dosanjh (1971). Values calculated according to S.A.E. international standards (1985) are also plotted. Experimental values of radiated acoustic power are correctly predicted by the two models. Figure 6b presents the experimental data of Lush (1971) and Tanna (1977). In addition, dimensional laws (Goldstein, 1976) for subsonic and supersonic jets are also plotted:

$$W \sim \rho_o D^2 \frac{U_j^8}{c_o^5} \frac{1 + M_c^2}{(1 - M_c^2)^4}$$

for a subsonic jet, and:

$$W \sim \rho_o D^2 U_j^3$$

for a supersonic jet.

One observes that the U_j^8 law closely follows variations of the acoustic power for a nominal Mach number $M \leq 1$, whereas the U_j^3 law is applicable for a nominal Mach number $M \leq 2$.

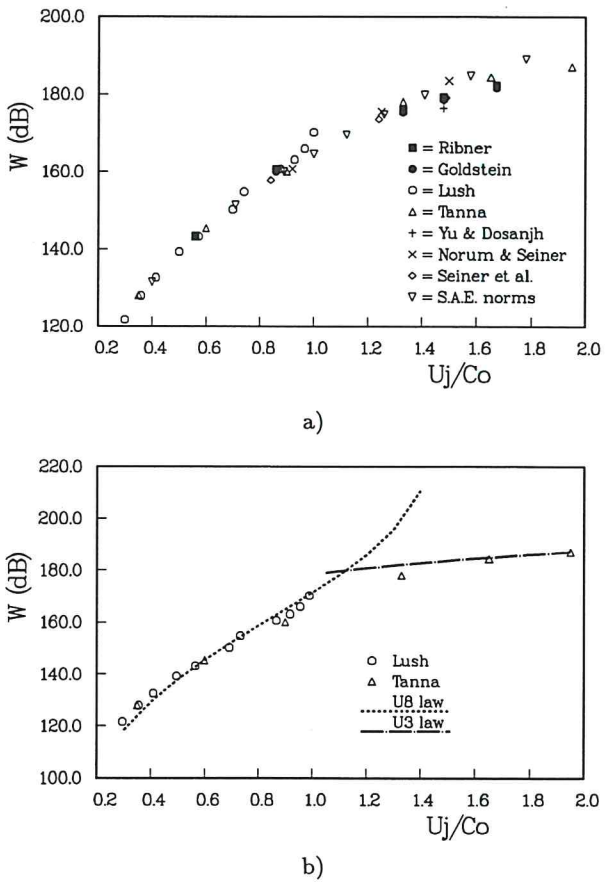

Figure 6. Evolution of acoustic power (dB - ref. 10^{-13} W) as a function of initial jet Mach number. (a) experimental data and calculated estimates, (b) experimental data and dimensional laws for subsonic and supersonic jets.

5.2.2. *Acoustic intensity*

Figures 7a to 7d display the acoustical intensity predicted by the two models, formulations (15, 16) and (23, 24), for a set of exhaust Mach numbers: 0.56, 0.86, 1.33 and 2.0. Intensity levels are expressed in dB with a reference of 10^{-12} W.m^{-2} , per unit of nozzle area. Numerical results are compared to experimental data of Lush for the case $M = 0.56$, Lush and Tanna for the case $M = 0.86$, and Tanna for the two cases $M = 1.33$ and $M = 2.0$.

Influence of the turbulence description is clearly shown in these figures. Ribner's model overestimates the noise level by 5 dB for small angles ($\theta \leq 30°$) unlike Goldstein's model. Secondly, we notice that the two models underestimate the intensity for rearward angles ($\theta \geq 90°$). This problem can be attributed to the simplified modeling adopted for convection. However, overall acoustic power can be accurately evaluated from the intensities determined at forward angles of observation ($\theta \leq 90°$). Goldstein's model demonstrates good agreement with experimental data for subsonic and moderate supersonic jets. The drop-off of experimental intensity for small angles is caused by refraction effects, which are not included in

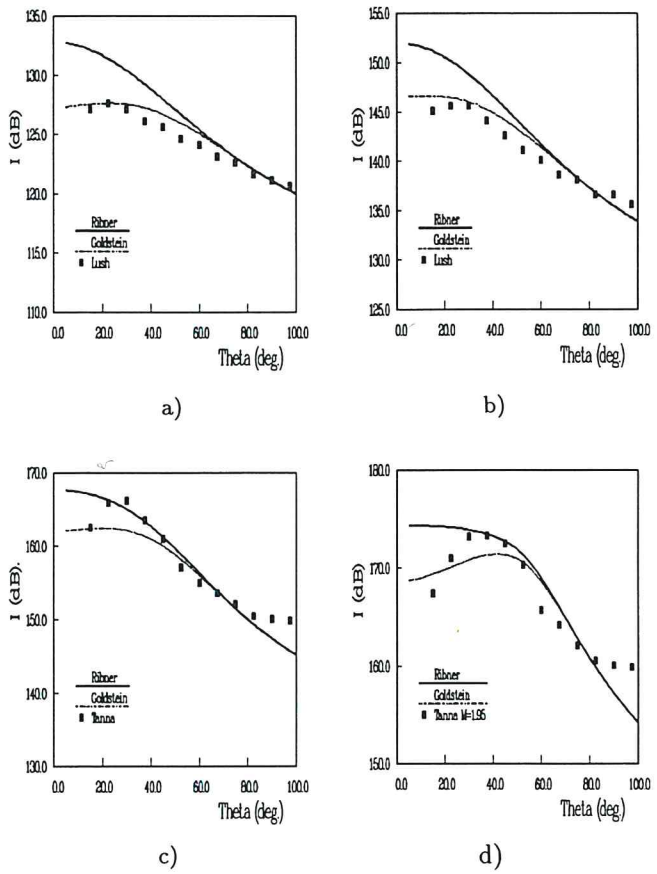

Figure 7. Radiated acoustic intensity (dB - ref. 10^{-12} W). (a) $M = 0.56$, (b) $M = 0.86$, (c) $M = 1.33$, (d) $M = 2.0$.

the models. Interpretation of the $M = 2.0$ case is more difficult. Indeed, difference of the directivity pattern between computations and experimental data becomes important. For this case, turbulent eddies are supersonically convected by the mean flow, with as a consequence an emission of eddy Mach waves. Unlike subsonic or moderate supersonic flows, turbulent eddies cannot be treated as compact sources and then, the evaluation of T_{ij} in Lighthill's analogy has to be carried out in a different way. Thus, one limitation of this approach is imposed by the sonic convection Mach number M_c , which corresponds to a nominal Mach number $M \simeq 1.5$.

5.2.3. $\frac{1}{3}$ - *octave spectra*

Third-octave spectra are plotted in Figure 8 as a function of the Strouhal number $S_t = fD/U_j$ for Ribner's model and for 4 nominal Mach number. Figures 8a, 8b and 8c respectively correspond to an observation angle θ of 90°, 120° and 15°. The numerical predictions are compared to experimental measurements of Tanna et al. (1976).

For the two cases $\theta = 90°$ and $\theta = 120°$, experimental values are correctly predicted with the numerical model. One finds that the model under-estimates the acoustic intensity for low Strouhal numbers ($S_t < 0.1$). In the third case $\theta = 15°$, one observes in measurements a translation of the spectral distribution of radiated energy because of refraction effects. However, in assuming that $T_{ij} = \rho_o u_i u_j$, one does not take into account these refraction effects, which become more important as acoustic source frequency increases. Refraction effects are particulary important in the forward arc and this explains the differences between predicted and measured third-octave spectra for $\theta = 15°$.

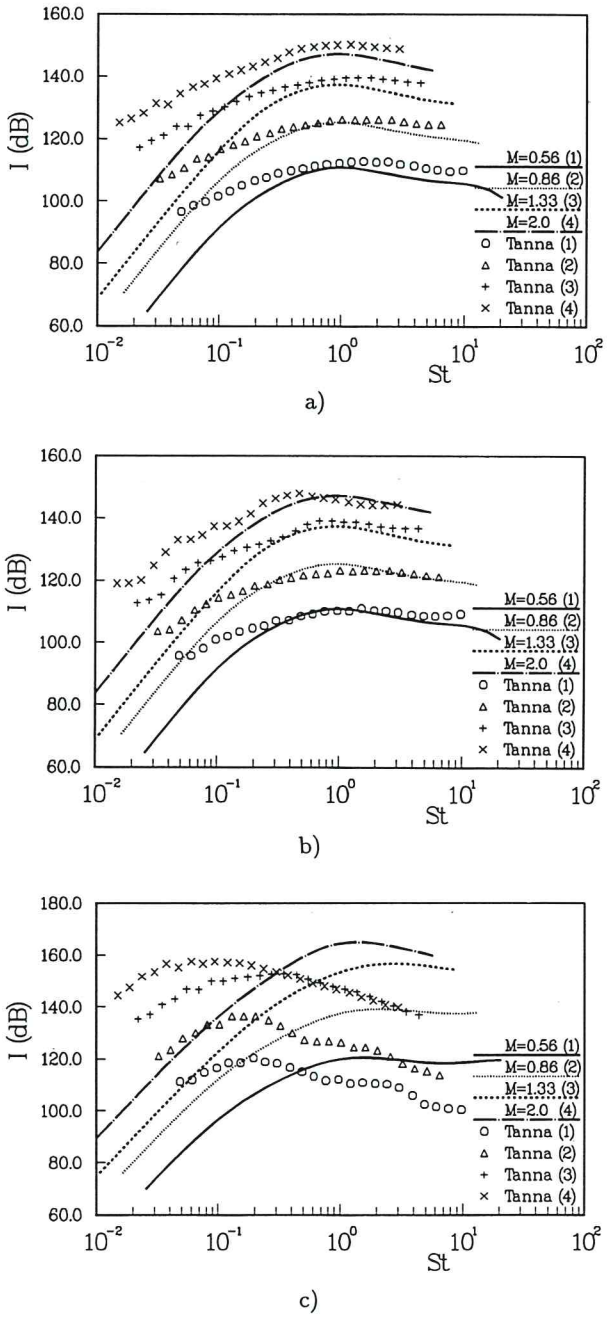

Figure 8. Third-octave band spectra. (a) $\theta = 90°$, (b) $\theta = 120°$, (c) $\theta = 15°$.

When refraction effects are negligible, one correctly retrieves the experimental data of Tanna, except for low

frequencies ($S_t < 0.1$). This lack of accuracy is due to the turbulence modeling ($k - \epsilon$ model) used in the aerodynamic computations.

5.2.4. *Space-frequency distributions of sound sources*

Space-frequency distributions of sound sources are plotted in Figure 9 for the three values of the Mach number $M = 0.86$, $M = 1.33$ and $M = 2.0$. One uses expression (25,26) of the Goldstein's model in reduced variables: $W_1/W_{1\max} = F(y^*, S_t)$ where $y^* = y_1/D$ is the dimensionless axial location, and S_t is the dimensionless frequency or Strouhal number of the source, which is given by :

$$S_t = \frac{\epsilon}{k}\frac{D}{U_j}$$

W_1 is the acoustic power per unit length of jet, deduced from the acoustic power by integration over the jet cross-section:

$$W_1(y_1) = \int\int_V W(\mathbf{y})\,dy_2 dy_3$$

Figure 9 indicates that sound sources are concentrated in the downstream region. The low frequency sources are located in the initial developed region, while the high frequency sources are situated in the mixing region, near the nozzle. Most of the acoustic power is emitted by the low wave-number components of turbulence. These results are in qualitative agreement with Lighthill's theory estimates (see for example Ffowcs Williams, 1963; Crighton, 1975; Goldstein, 1976). The maximum of the acoustic power moves downstream as the Mach number increases ($y^* = 7.2$ for $M = 0.86$, $y^* = 8.4$ for $M = 1.33$, $y^* = 12.3$ for $M = 2.0$). This shift is due to the growth of the potentiel core and to the associated displacement of the regions where turbulent kinetic energy is produced.

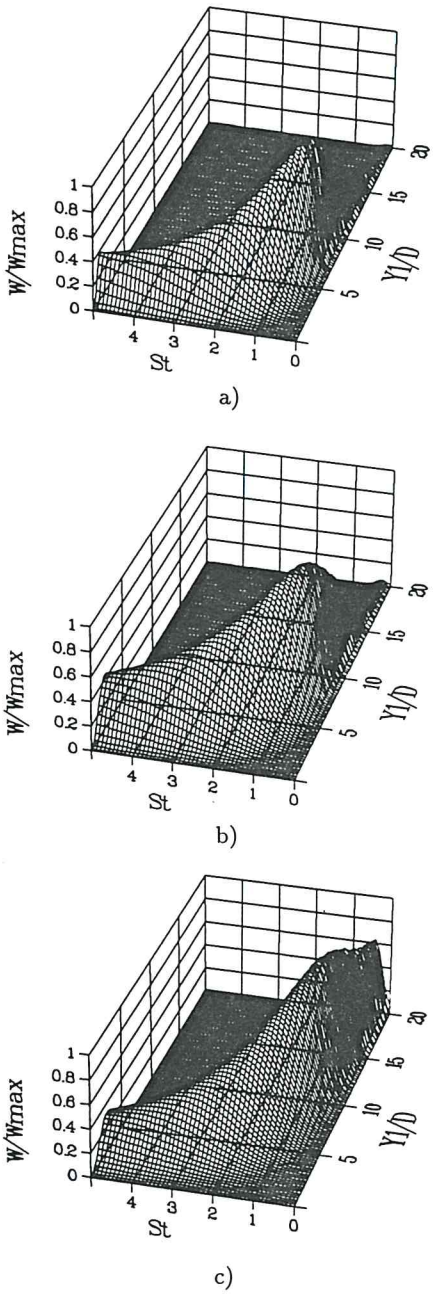

Figure 9. Space-frequency distribution of sound sources. (a) $M = 0.86$, (b) $M = 1.33$, (c) $M = 2.0$.

6. Conclusion

We develop in this article a numerical method for the determination of jet noise based on extensions of Lighthill's theory. Aerodynamic calculations are carried out using a $k - \epsilon$ turbulent code, modified for compressible shear flows. Two formulations of noise generated aerodynamically are studied: Ribner's model (1969), which assumes an isotropic description of the turbulence, and Goldstein & Rosenbaum's model which assumes an axisymmetric description of the turbulence. These models have been modified in order to incorporate statistical information about the turbulence from local aerodynamic results. The models use as input the calculated mean velocity, turbulent kinetic energy k, and the rate of dissipation ϵ . The two models are in good agreement with experimental data for the evolution of acoustic power as a function of the jet exit velocity. However, Goldstein's model yields more accurate predictions of the directivity pattern. One also obtains with this approach a complete picture of the space-frequency distributions of sound sources in the jet. On this basis it appears that similar calculations could be used to deal with others jet geometries, such as coaxial jets (see Béchara, 1992; Béchara et al., 1992, 1993). In a more general flow configuration, this approach still has three limitations. First, it requires a specific Green's function which uses the integral formulation of the Lighthill's equation. Secondly, refraction effects due to mean flow gradients are not taken into account but they are known to modify the aerodynamic noise spectrum. Third, the convection Mach number must remain in the subsonic

range or else the acoustic field is dominated by emission of eddy Mach waves.

Appendix A

Turbulence model equations - The ESTET code

The basic mean flow equations which are solved numerically are given in the following section. Then, the modified $k-\epsilon$ turbulence model for compressible mixing layers is decribed in the next Section. Finally, the ESTET code is briefly presented in the last Section.

A.1. *Mean flow equations*

A density-weighted (Favre) average is often used for compressible flows. With this averaging precedure, the conservation equations of mass and momentum take a similar form as in the incompressible case. Then, using the Favre average for each variable $\phi = \tilde{\phi} + \phi'' = \overline{\rho\phi}/\overline{\rho} + \phi''$, except for the density and pressure, one may write the mean flow equations as follows:

1. continuity equation

$$\frac{\partial \overline{\rho}}{\partial t} + \frac{\partial (\overline{\rho}\tilde{u}_i)}{\partial x_i} = 0$$

2. momentum conservation equation

$$\overline{\rho}\left(\frac{\partial \tilde{u}_i}{\partial t} + \tilde{u}_j \frac{\partial \tilde{u}_i}{\partial x_j}\right) = -\frac{\partial \overline{p}}{\partial x_j} + \frac{\partial}{\partial x_j}\left(\overline{\tau_{ij}} - \overline{\rho u''_i u''_j}\right)$$

where τ_{ij} is the viscous stress tensor, which takes the following form for a compressible newtonian fluid:

$$\tau_{ij} = \mu\left(\frac{\partial u_i}{\partial x_j} + \frac{\partial u_j}{\partial x_i}\right) - \frac{2}{3}\mu\frac{\partial u_k}{\partial x_k}\delta_{ij}$$

and $-\overline{\rho u''_i u''_j}$ is the turbulence Reynolds stresses.

A.2. *Turbulence model*

A modified $k-\epsilon$ turbulence model for compressible mixing layers is used to calculate the Reynolds stresses. The modification concerns the dissipation ϵ and is based on works of Zeman (1990). In this Section, we only present the finally form of the $k-\epsilon$ turbulence model.

The kinetic energy k is given by:

$$k = \frac{1}{2}\widetilde{u''_i u''_i}$$

The dissipation ϵ of this kinetic energy is the sum of two contributions $\epsilon = \epsilon_s + \epsilon_d$. ϵ_s is the solenoidal dissipation associated with the incompressible part of the velocity field. The distribution of this dissipation is given by the standard transport equation for the dissipation. The dilatation dissipation ϵ_d resulting from dilatation effects of the velocity field is given by the following expression proposed by Zeman:

$$\epsilon = \epsilon_s + \epsilon_d = \epsilon_s\left[1 + c_d f\left(M_t\right)\right]$$

with $M_t = \frac{\sqrt{2k}}{c}$ and $c_d = 0.75$

with the following function f:

$$\begin{cases} f(M_t) = 1 - \exp\left[-\left(\frac{M_t - 0{,}1}{0{,}6}\right)^2\right] & \text{if } M_t > 0{,}1 \\ f(M_t) = 0 & \text{if } M_t \leq 0{,}1 \end{cases}$$

The transport equations for k and ϵ take the following form:

$$\overline{\rho}\left(\frac{\partial k}{\partial t} + \tilde{u}_j\frac{\partial k}{\partial x_j}\right) = \\ = \frac{\partial}{\partial x_j}\left[\left(\mu + \frac{\mu_t}{\sigma_k}\right)\frac{\partial k}{\partial x_j}\right] + \mathbf{P} + \mathbf{G} - \overline{\rho}\epsilon$$

$$\overline{\rho}\left(\frac{\partial \epsilon_s}{\partial t} + \tilde{u}_j\frac{\partial \epsilon_s}{\partial x_j}\right) = \\ = \frac{\partial}{\partial x_j}\left[\left(\mu + \frac{\mu_t}{\sigma_\epsilon}\right)\frac{\partial \epsilon_s}{\partial x_j}\right] + \frac{\epsilon_s}{k}\left[C_{\epsilon 1}\left(\mathbf{P} + \mathbf{G}\right) - C_{\epsilon 2}\overline{\rho}\epsilon_s\right]$$

Using the eddy viscosity concept, which relates the Reynolds stresses to the mean flow gradients, the production term $\mathbf{P}$ may be written as:

$$\mathbf{P} = -\overline{\rho u''_i u''_j}\frac{\partial \tilde{u}_i}{\partial x_j} \\ = \left[\mu_t\left(\frac{\partial \tilde{u}_i}{\partial x_j} + \frac{\partial \tilde{u}_j}{\partial x_i} - \frac{2}{3}\frac{\partial \tilde{u}_k}{\partial x_k}\delta_{ij}\right) - \frac{2}{3}\overline{\rho}k\delta_{ij}\right]\frac{\partial \tilde{u}_i}{\partial x_j}$$

where μ_t is the turbulent viscosity given by:

$$\mu_t = \overline{\rho}C_\mu\frac{k^2}{\epsilon}$$

The other production term $\mathbf{G}$ is calculated as (Jones, 1979):

$$\mathbf{G} = \frac{\overline{\rho' u''_i}}{\overline{\rho}}\frac{\partial \overline{p}}{\partial x_i} = -\frac{1}{\overline{\rho}}\frac{\mu_t}{\sigma_t}\frac{\partial \overline{\rho}}{\partial x_i}\frac{\partial \overline{p}}{\partial x_i} \qquad \text{with} \qquad 0.7 \leq \sigma_t \leq 1.$$

The standard values of the empirical constants of the $k-\epsilon$ model given by Launder and Spalding (1974) are used in the calculations:

$$C_\mu = 0.09 \quad C_{\epsilon 1} = 1.44 \quad C_{\epsilon 2} = 1.92$$
$$\sigma_k = 1.0 \quad \sigma_\epsilon = 1.3$$

A.3. *The ESTET code*

The ESTET code has been developed by the "Laboratoire National Hydraulique" of the "Direction des Etudes et Recherches d'Electricité de France". The algorithm is based on the projection method, introduced by Chorin & Temam (1967), for the time discretization of the Navier-Stokes equations. The characteristic method is used for the convection step. The diffusion step and the pressure-continuity step (or projection step) are solved using implicit methods. The global method is of first-order accuracy.

The mesh is structured but irregular and all the calculations are performed with an axisymetric version of ESTET.

Appendix B

Nomenclature

c	sound speed
C	convection factor $C = 1 - M_c \cos\theta$
C_{pp}	autocorrelation function of the pressure
D	nozzle diameter
k	turbulent kinetic energy
L	Integral scale length of turbulence
M_c	convection Mach number $M_c = U_c/c_o$
M	nominal Mach number $M = U_j/c_o$
p	pressure
S_{pp}	power spectral density of the acoustic intensity
T_{ij}	Lighthill's stress tensor
t	time
u	velocity
u_t	fluctuating turbulent velocity
U	mean flow velocity
U_c	eddy convection velocity
U_j	jet exit velocity
W	radiated acoustic power
$\mathbf{x}$	coordinates of the observation point
$\mathbf{y}$	coordinates of the current source point
δ_{ij}	Kronecker delta
ϵ	rate of dissipation of the turbulent kinetic energy k
θ	angle between the mean flow direction and the observer $\cos\theta = \mathbf{x}.\mathbf{y_1}/x$
η	vector which separates two points in the source volume in the fixed frame
ξ	vector which separates two points in the source volume in the moving frame
ρ	density
τ_{ij}	viscous stress tensor
ω_f	local characteristic angular frequency of turbulence

Subscripts

o	value of quantity in the medium at rest
1	value of quantity in the axial direction, which is the mean flow direction
2	value of quantity in the radial direction
$'$	value of quantity at the point $(\mathbf{y}, t)$
$''$	value of quantity at the point $(\mathbf{y}+\boldsymbol{\eta}, t+\tau)$

The origin of coordinate system is taken within the source volume V .

References

BATCHELOR G.K. (1953) "The theory of homogeneous turbulence", Cambridge University Press

BECHARA W. (1992) "Modélisation du bruit d'écoulements turbulents libres", Thèse de doctorat, Ecole Centrale Paris, 1992-02

BECHARA W., LAFON P., CANDEL S. (1992) "Application of a $k-\epsilon$ model to the prediction of noise for simple and coaxial free jets", J. Acout. Soc. Am., submitted for publication

BECHARA W., LAFON P., CANDEL S. (1993) "Modélisation du bruit des jets turbulents libres et subsoniques à température ambiante", J. Phys. III France, 3, 653-674

CRIGHTON D. (1975) "Basic principles of aerodynamic noise generation", Prog. Aerospace Science, 16(1), 31-96

DAVIES P.O.A.L., FISHER M.J., BARATT M.J. (1963) "The characteristics of the turbulence in the mixing region of a round jet", J. Fluid Mech., 15(3), 337-367

DOAK P.E. (1972) "Analysis of internally generated sound in continuous materials: 2. A critical review of the conceptual adequacy and physical scope of existing theories of aerodynamic noise, with special reference to supersonic jet noise", J. Sound Vibration, 25(2), 263-335

FFOWCS WILLIAMS J.E. (1960) "Some thoughts on effects of aircraft motion and eddy convection on the noise from air jets", University of Southampton, AASU Report 155

FFOWCS WILLIAMS J.E. (1963) "The noise from turbulence convected at high speed", Philos. Trans. Royal Soc. London, 255, Ser.A, 469-503

GOLDSTEIN M.E., ROSENBAUM B. (1973) "Effect of anisotropic turbulence on aerodynamic noise", J. Acoust. Soc. Am., 54(3), 630-645

GOLDSTEIN M.E. (1976) "Aeroacoustics", McGraw-Hill International Book Compagny, New York

HINZE J.O. (1975) "Turbulence, second edition", McGraw-Hill International Book Compagny, New York

JONES W.P. (1979) "Prediction methods for turbulent flows", Von Karman Institute for Fluid Dynamics, Lecture series 1979-2

LAUNDER B.E., SPALDING D.B. (1974) "The numerical computation of turbulent flows", Computer Methods in Applied Mechnical Engineering, 3(2), 269-289

LAU J.C., MORRIS P.J., FISHER M.J. (1979) "Measurements in subsonic and supersonic free jets using a laser velocimeter", J. Fluid Mech., 93(1), 1-27

LIGHTHILL M.J. (1952) "On sound generated aerodynamically - I. General theory", Proc. of the Royal Society of London, Vol. 211, Ser. A, 1107, 564-587

LIGHTHILL M.J. (1954) "On sound generated aerodynamically - II. Turbulence as a source of sound", Proc. of the Royal Society of London, Vol. 222, Ser. A, 1148, 1-32

LILLEY G.M. (1958) "On the noise from air jets", Aeronautical Research Council (Great Britain), A.R.C. 20-276

LILLEY G.M. (1972) "The generation and radiation of supersonic jet noise. Vol. IV - Theory of turbulence generated jet noise, noise radiation from upstream sources, and combustion noise. Part II: Generation of sound in a mixing region", Air Force Aero Propulsion Laboratory, AFAPL-TR-72-53

LUSH P.A. (1971) "Measurements of subsonic jet noise and comparison with theory", J. Fluid Mech., 46(3), 477-500

NAGAMATSU H.T., SHEER J., GILL M.S. (1970) "Flow and acoustic characteristics of subsonic and supersonic jets from convergent nozzle", 3rd Fluid and Plasma Dynamics Conference, Los Angeles, California

NORUM T.D., SEINER J.M. (1982) "Measurements of mean static pressure and far field acoustics of shock containing supersonic jets", NASA TM 84521

PAO S.P., LOWSON M.V. (1970) "Some applications of jet noise theory", 8th Aerospace Sciences Meeting, New York AIAA Paper 70-223, 38(1), 1-24

PHILLIPS O.M., (1960) "On the generation of sound by supersonic turbulent shear layers", J. Fluid Mech., 9(1), 1-28

PROUDMAN I. (1952) "The generation of sound by isotropic turbulence", Proc. of the Royal Society of London, Vol. A, 214, 119-132

RIBNER H.S. (1964) "The generation of sound by turbulent jets", Academic Press, New York, 103-182

RIBNER H.S. (1969) "Quadripole correlations governing the pattern of jet noise", J. Fluid Mech., 38(1), 1-24

S.A.E. (1985) "Gas turbine exhaust noise predictions", ARP 876C

SEINER J.M., McLAUGHLIN D.K., LIU C.H. (1982) "Supersonic jet noise generated by large scale instabilities", NASA, Technical Paper 2072

TANNA H.K., DEAN P.D., BURRIN R.H. (1976) "The generation and radiation of supersonic jet noise, Vol.III Turbulent mixing noise data", Air Force Aero-Propulsion Laboratory, AFAPL-TR-76-65

TANNA H.K. (1977) "An experimental study of jet noise, Part I: turbulent mixing noise", J. Sound Vibration, 50(3), 405-428

YU J.C., DOSANJH D.S. (1971) "Noise field of a supersonic Mach 1.5 cold jet", J. Acoust. Soc. Am., 51, 1400-1410

ZEMAN O. (1990) "Dilatation-dissipation: the concept and application in modeling compressible mixing layers", Phys. Fluid A, 2(2), 178-188